

# Deep Learning-based Deconvolution for Astronomical Surveys

Utsav Akhaury

Pascale Jablonka, Jean-Luc Starck, Frédéric Courbin

**EPFL**





European Space Agency



VERA C. RUBIN OBSERVATORY

See the Universe in action  
Rubin Observatory will answer some of our biggest questions about the Universe!

Press Release

Rubin Observatory Will Help Unravel Mysteries of Dark Matter and Dark Energy

THE EUROPEAN SPACE AGENCY

SCIENCE & EXPLORATION

euclid

Exploring the dark Universe



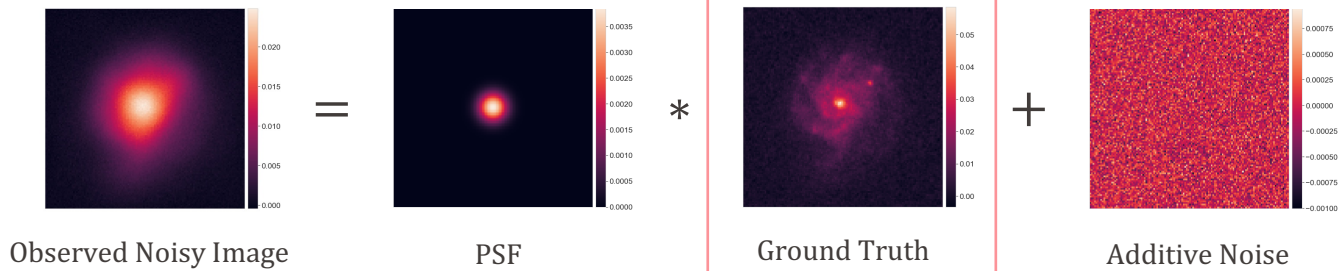
# Introduction & Motivation

- Need to be better understand phenomena in galaxy formation & evolution:
  - mechanism of inflow/outflow
  - position of galaxies in the cosmic web and their evolution
  - the importance of mergers
  - star formation and mass maps in high resolution
  - star formation rate
- Multi-wavelength images over a wide field of view only available from **ground-based** telescopes
  - **Degraded** due to atmospheric blurring and instrumental optics
- Access to clear **high-resolution** images
  - Increasing need to develop **fast** and **accurate** deconvolution algorithms that generalize well
-

# The Deconvolution Problem

## Model

$$\mathbf{y} = \mathbf{h} * \mathbf{x}_t + \boldsymbol{\eta}$$



$$\mathbf{y} \in \mathbb{R}^{n \times n}$$

$$\mathbf{x}_t \in \mathbb{R}^{n \times n}$$

$$\mathbf{h} \in \mathbb{R}^{n \times n}$$

$$\boldsymbol{\eta} \in \mathbb{R}^{n \times n}$$

- Observed Noisy Image
- Ground Truth Image
- PSF
- Additive Noise

## Issues

- The equation is **ill-conditioned** and **ill-posed**
- Problem could be handled by regularization

# The Deconvolution Step

## Loss Function

$$L(\mathbf{x}) = \frac{1}{2\sigma^2} \|\mathbf{H}\mathbf{x} - \mathbf{y}\|_2^2 + \lambda \|\mathbf{\Gamma}\mathbf{x}\|_2^2$$

## Tikhonov Deconvolution

$$\hat{\mathbf{x}} = (\mathbf{H}^\top \mathbf{H} + \lambda \mathbf{\Gamma}^\top \mathbf{\Gamma})^{-1} \mathbf{H}^\top \mathbf{y}$$

$\sigma \in \mathbb{R}$

$\mathbf{\Gamma} \in \mathbb{R}^{n^2 \times n^2}$

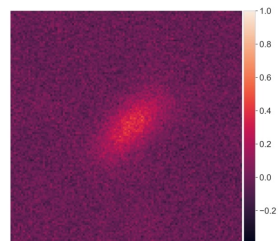
$\lambda \in \mathbb{R}_+$

$\mathbf{H} \in \mathbb{R}^{n^2 \times n^2}$

- Noise standard deviation
- Linear Tikhonov filter set to a Laplacian high-pass filter (to penalize high frequencies)
- Regularization weight
- Block circulant matrix associated with the convolution operator  $\mathbf{h}$

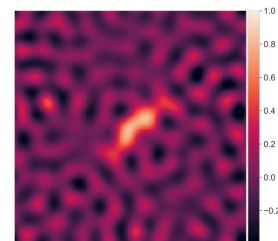
$\mathbf{y}$

Convolved Noisy Image



$\hat{\mathbf{x}}$

Tikhonov Solution



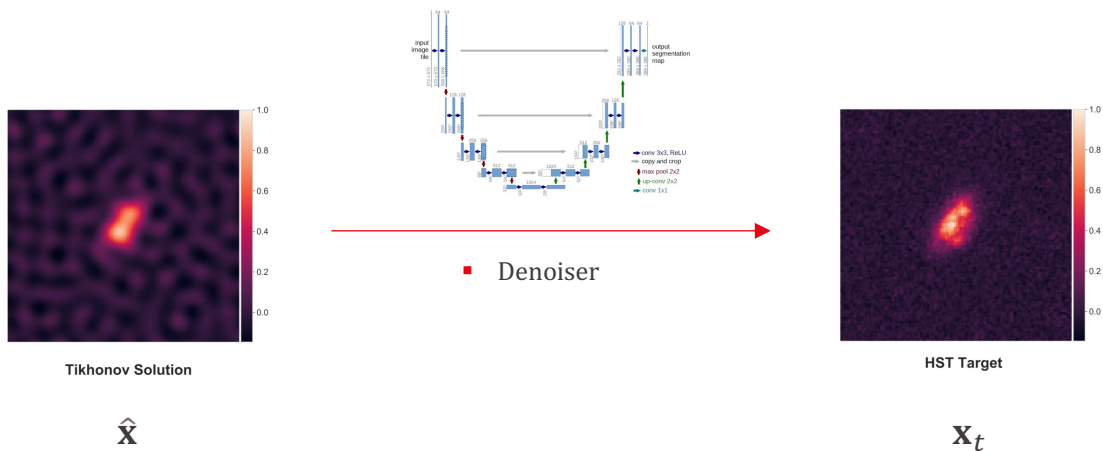
Tikhonov output contains correlated noise



# The Denoising Step

The training is aimed to make the network learn the following mapping while minimizing a suitable loss function:

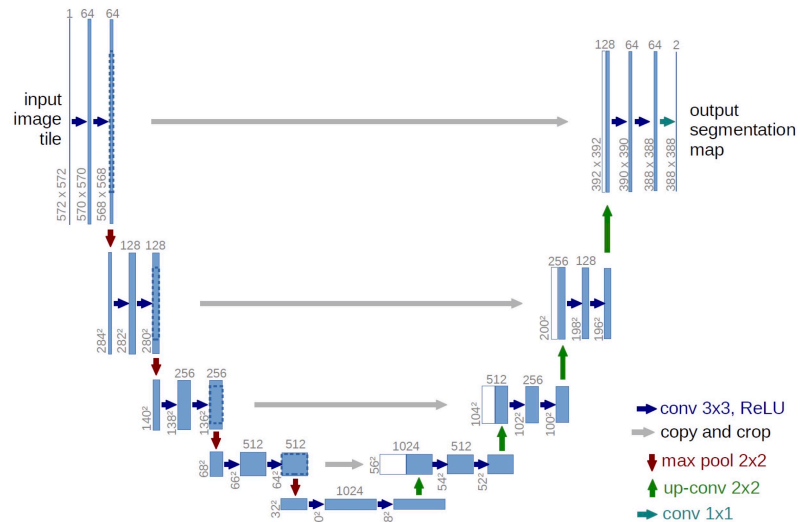
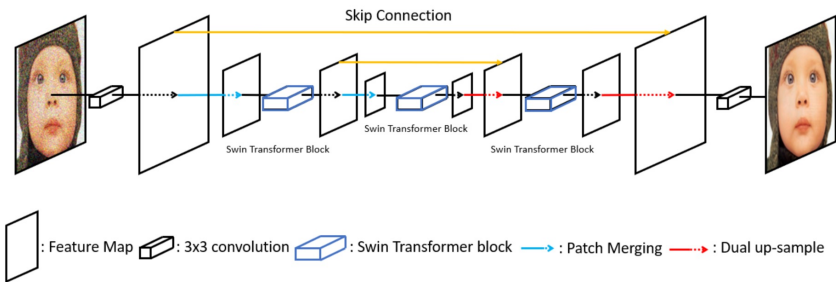
- Tikhonov output  $\hat{\mathbf{x}}$   $\longrightarrow$  ground truth image  $\mathbf{x}_t$



# U-net

- Originally developed for biomedical image segmentation
- Relevant to many other imaging problems, like **denoising**
- U-nets consist of a multi-scale approach, allowing the signal to be analyzed at multiple resolutions

# SUNet

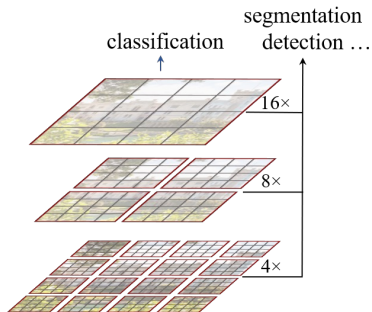


U-Net: Convolutional Networks for Biomedical Image Segmentation  
 Ronneberger et al, 2015

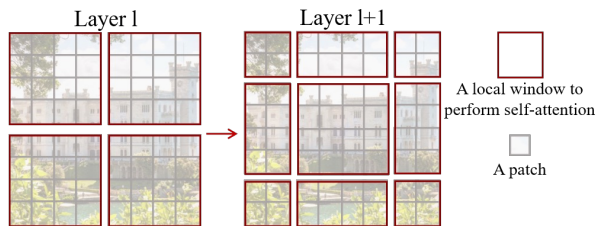
- A Unet with **Swin Transformer** blocks incorporated in the architecture

SUNet: Swin Transformer UNet for Image Denoising,  
 Fan et al, 2022

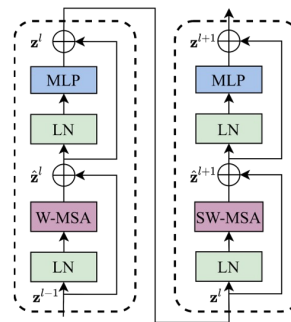
# Swin Transformer



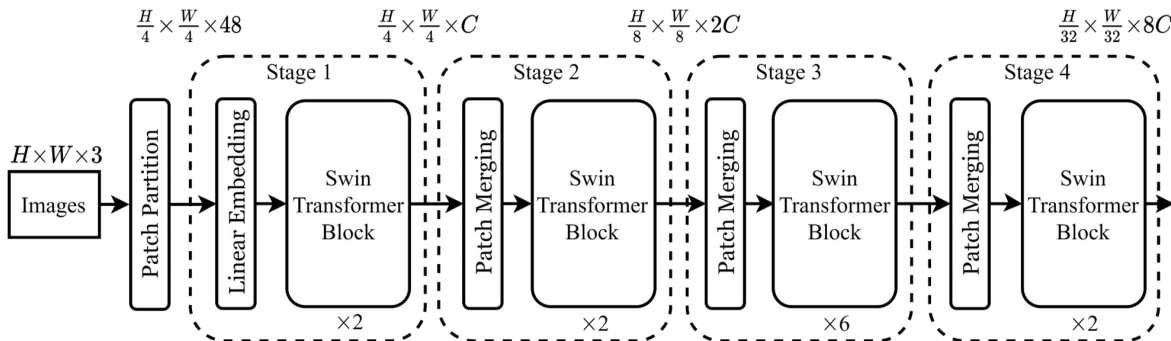
(a) Swin Transformer



(b) Shifted Window



(c) Two Successive Swin Transformer Blocks

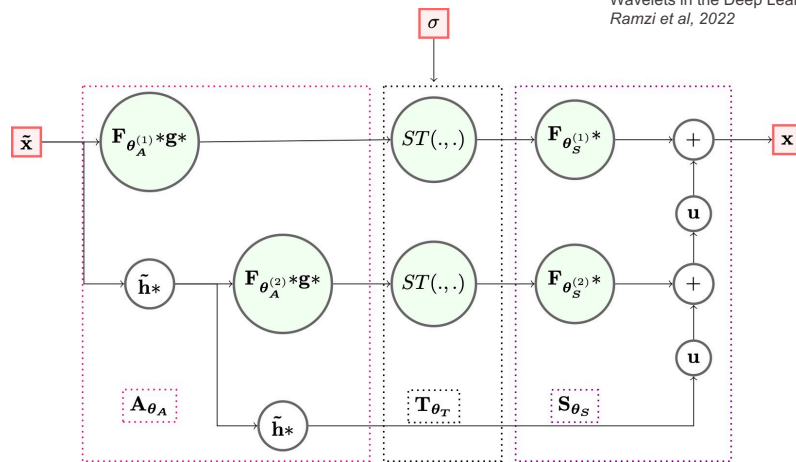


(d) Architecture



# Learnlet

- The Learnlet decomposition (Ramzi et al, 2021) aims at learning a filter bank in a denoising setting with backpropagation and gradient descent
- Learnlets exploit the best of both of deep learning and classical algorithms –
  - uses gradient descent to improve the expressive power of wavelets
  - preserves some interesting wavelet properties like exact reconstruction
- $m = 5$  scales  $\rightarrow$  44,840 trainable parameters  
 $128 \times 128$



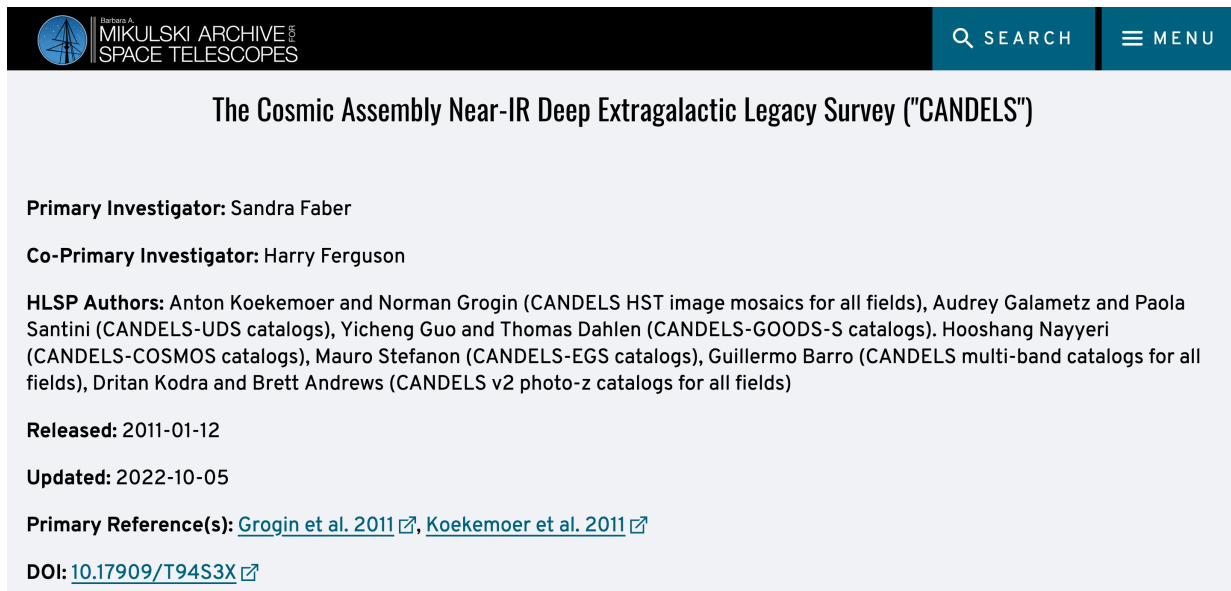
$$\mathbf{f}_{\theta}(\tilde{\mathbf{x}}, \sigma) = \mathbf{S}_{\theta_S} \left( \mathbf{T}_{\theta_T} \left( \mathbf{A}_{\theta_A}(\tilde{\mathbf{x}}), \sigma \right) \right) : (\mathbb{R}^{n \times n} \times \Sigma) \rightarrow \mathbb{R}^{n \times n}$$

- $\Sigma$  ▪ set of possible values for the noise standard deviation  $\sigma$
- $m$  ▪ Number of scales
- $\theta = (\theta_S, \theta_T, \theta_A) \in \Theta_m$  ▪ a given set of parameters

# Dataset Generation & Training

## Ground Truth Images

- CANDELS – Five different image mosaics (GOODS-N, GOODS-S, EGS, UDS, COSMOS)
- HST cutouts of  $128 \times 128$  pixels from CANDELS in the *F606W* filter (*V*-band) centred at the object centroid



The screenshot shows the MAST website interface. At the top left is the MAST logo with the text "Barbara A. MIKULSKI ARCHIVE FOR SPACE TELESCOPES". To the right are "SEARCH" and "MENU" buttons. The main heading is "The Cosmic Assembly Near-IR Deep Extragalactic Legacy Survey ('CANDELS')". Below this, the "Primary Investigator" is Sandra Faber, and the "Co-Primary Investigator" is Harry Ferguson. The "HLSP Authors" section lists Anton Koekemoer and Norman Grogin (CANDELS HST image mosaics for all fields), Audrey Galametz and Paola Santini (CANDELS-UDS catalogs), Yicheng Guo and Thomas Dahlen (CANDELS-GOODS-S catalogs), Hooshang Nayyeri (CANDELS-COSMOS catalogs), Mauro Stefanon (CANDELS-EGS catalogs), Guillermo Barro (CANDELS multi-band catalogs for all fields), Dritan Kodra and Brett Andrews (CANDELS v2 photo-z catalogs for all fields). The "Released" date is 2011-01-12, and the "Updated" date is 2022-10-05. The "Primary Reference(s)" are Grogin et al. 2011 and Koekemoer et al. 2011. The DOI is 10.17909/T94S3X.

Barbara A. MIKULSKI ARCHIVE FOR SPACE TELESCOPES

SEARCH MENU

## The Cosmic Assembly Near-IR Deep Extragalactic Legacy Survey ("CANDELS")

**Primary Investigator:** Sandra Faber

**Co-Primary Investigator:** Harry Ferguson

**HLSP Authors:** Anton Koekemoer and Norman Grogin (CANDELS HST image mosaics for all fields), Audrey Galametz and Paola Santini (CANDELS-UDS catalogs), Yicheng Guo and Thomas Dahlen (CANDELS-GOODS-S catalogs), Hooshang Nayyeri (CANDELS-COSMOS catalogs), Mauro Stefanon (CANDELS-EGS catalogs), Guillermo Barro (CANDELS multi-band catalogs for all fields), Dritan Kodra and Brett Andrews (CANDELS v2 photo-z catalogs for all fields)

**Released:** 2011-01-12

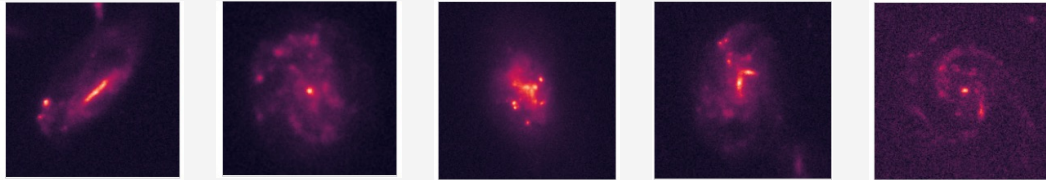
**Updated:** 2022-10-05

**Primary Reference(s):** [Grogin et al. 2011](#), [Koekemoer et al. 2011](#)

**DOI:** [10.17909/T94S3X](https://doi.org/10.17909/T94S3X)

# Filtering

- Selected good galaxy candidates and excluded point-sized objects using the following filtering criteria:
  - $MAG\_AUTO < 26$  (AB magnitude in SExtractor "AUTO" aperture)
  - $Flux\_Radius_{80} > 10$  (80% enclosed flux radius in pixels)
  - $FWHM > 10$  (full width at half maximum in pixels)



Good Candidates



Rejected



## Noisy Simulations

- Convolved  $\sim 25,000$  ground-truth images with a Gaussian PSF having an FWHM of 15 pixels
- Added white Gaussian noise with a standard deviation  $\sigma_{noise}$  having a value such that the faintest object in our dataset has a peak SNR close to 1
- Train-Validation-Test split – 0.8 : 0.1 : 0.1

## Normalization

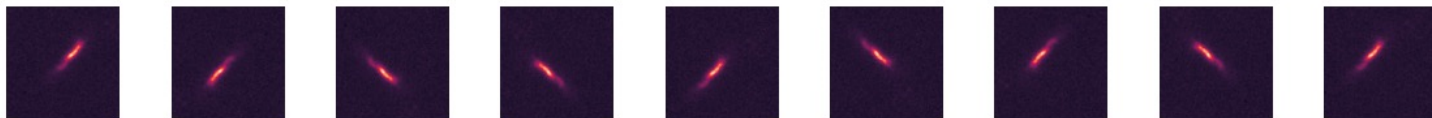
- Normalized each image  $\mathbf{x}_{(i)}$  by subtracting its mean  $\mu_{(i)}$  and scaling within the  $[-1, 1]$  range as follows:

$$\frac{\mathbf{x}_{(i)} - \mu_{(i)}}{\max[\mathbf{x}_{(i)}^t - \mu_{(i)}^t]}$$

- $\mathbf{x}_{(i)}^t$  -  $i^{th}$  target image
- $\mu_{(i)}^t$  - mean of  $i^{th}$  target image

## Data Augmentation

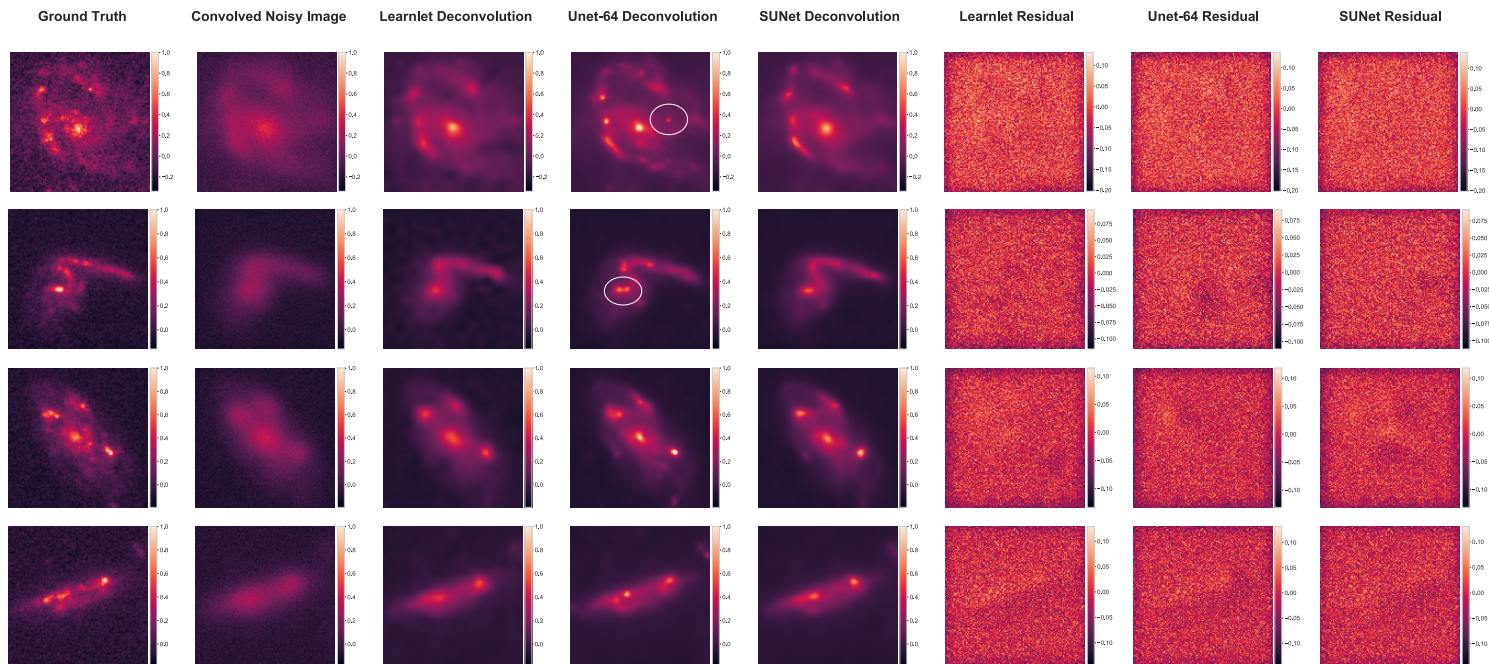
- Random rotations in multiples of  $90^\circ$ , translations and flips along horizontal & vertical axes



# Performance Comparison

Method	No. of parameters	Batch Size	Epochs	Training Time (hrs.)	Runtime per image (ms)
Learnlet	44,840	32	150	5.45	30.8
Unet-64	31,023,940	32	500	14.4	26.3
SUNet	38,365,111	16	250	90	15.2

All computations  
on Titan RTX  
Turing GPU with  
24 GB RAM



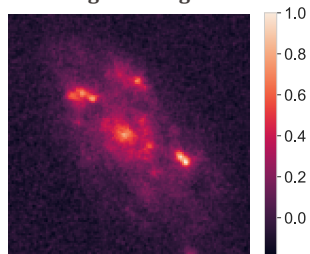
# Results

$$\text{Residual} = \mathbf{y} - \mathbf{h} * N_{\theta}(\hat{\mathbf{x}})$$

- $\mathbf{y}$  - noisy image
- $\mathbf{h}$  - PSF
- $\hat{\mathbf{x}}$  - noisy tikhonov input
- $N_{\theta}$  - network model

# Multi-resolution Analysis

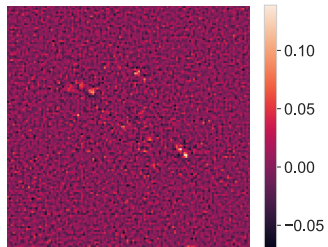
Original Image



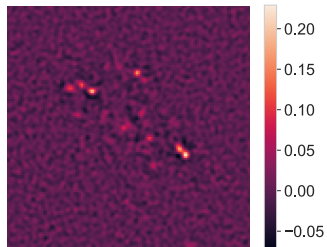
- Wavelet decomposition using SCARLET



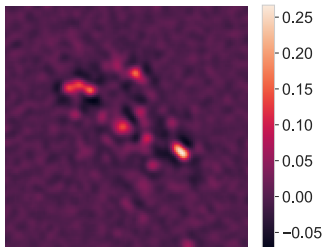
Scale 1



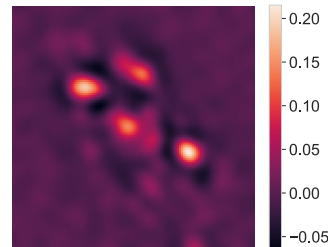
Scale 2



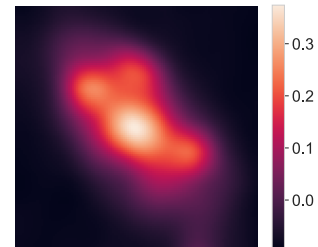
Scale 3



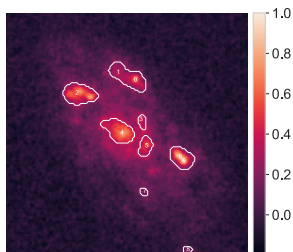
Scale 4



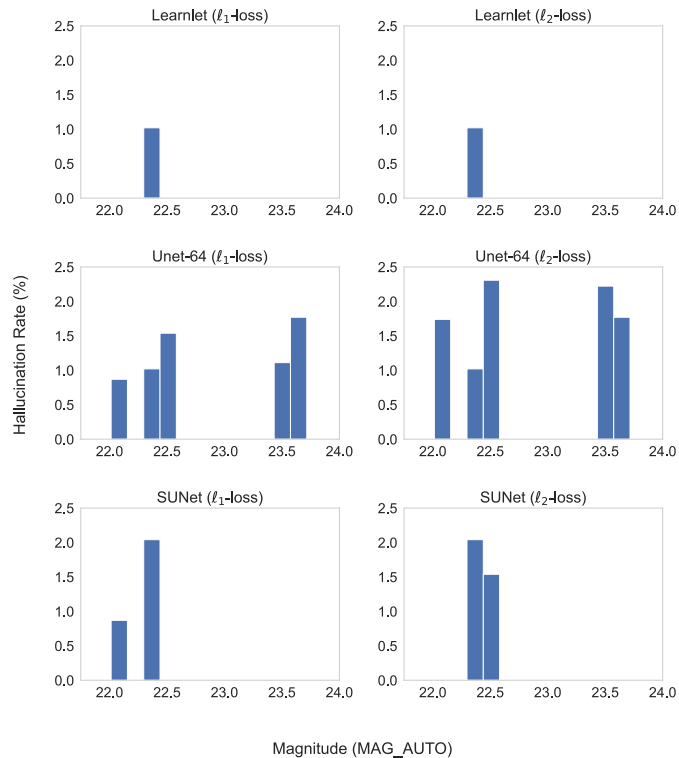
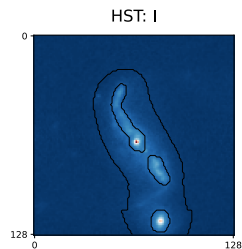
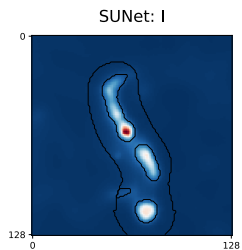
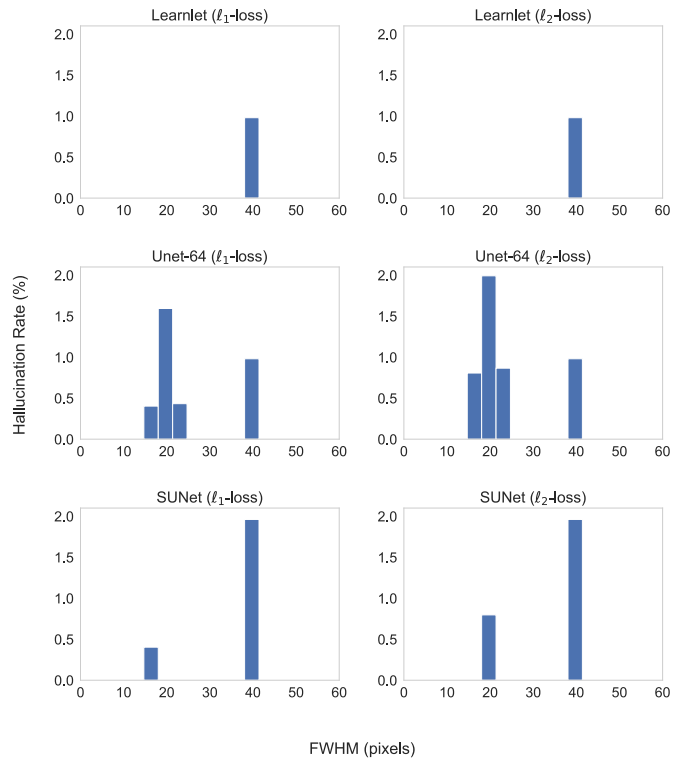
Scale 5



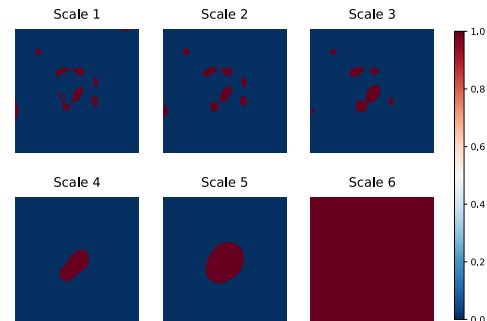
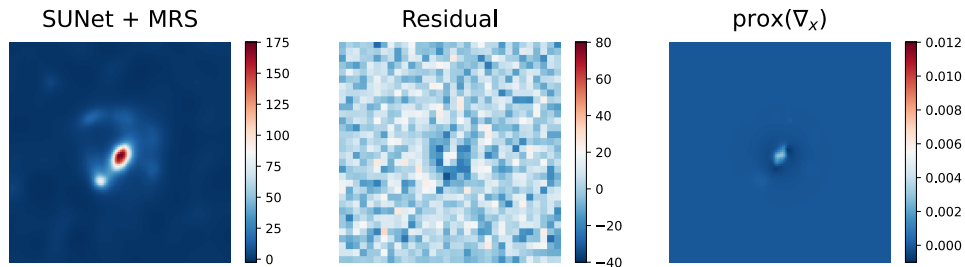
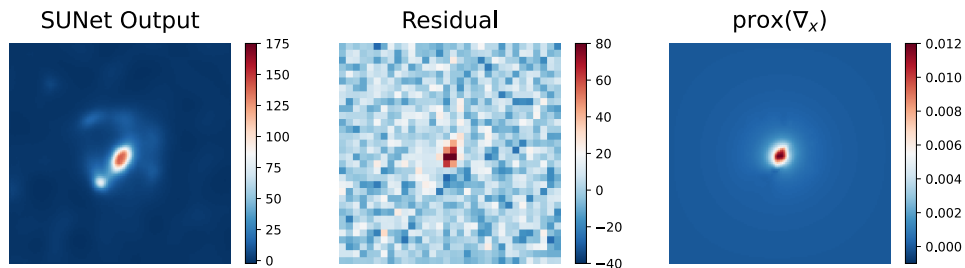
3<sup>rd</sup> Scale selected to detect clumps



# Hallucination Rate



# Debiasing with Multi-resolution Support (MRS)



$$\mathbf{x}_{j+1} = \mathbf{x}_j + \text{prox}(\nabla_x)$$

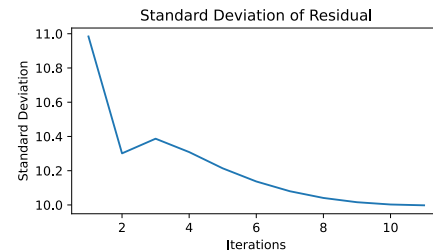
where

$$\mathbf{r}_j = \mathbf{y} - \mathbf{H}\mathbf{x}_j$$

$$\nabla_x = \mathbf{H}^\top \mathbf{r}_j$$

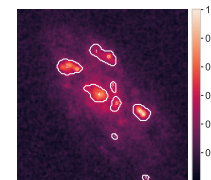
$$\text{prox}(\nabla_x) = (\Phi^\top \mathbf{M} \Phi) \nabla_x$$

$$\mathbf{M} = \text{MRS}(\Phi(\mathbf{x}_0))$$

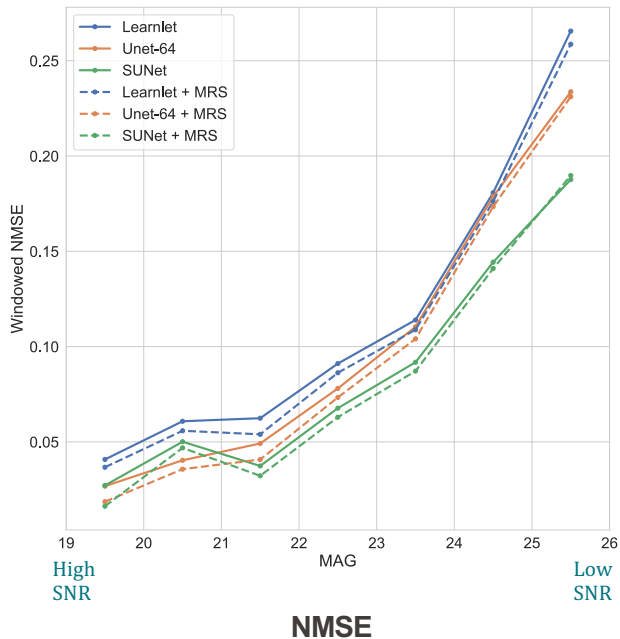


# Metrics

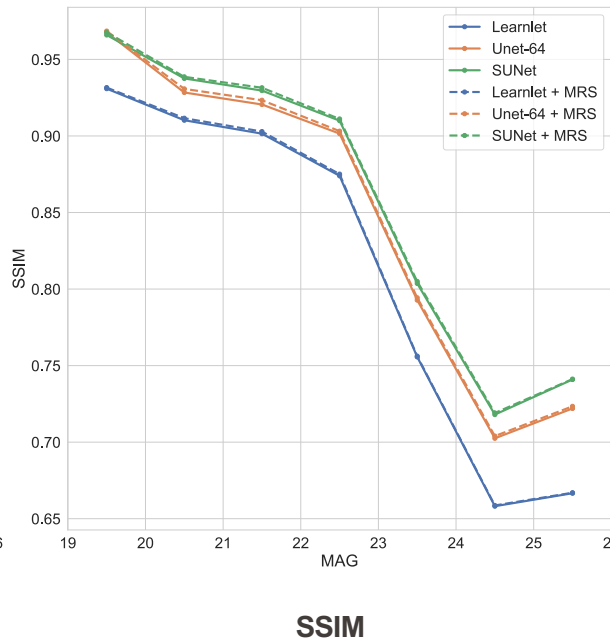
Extracted Flux in  
small-scale  
structures



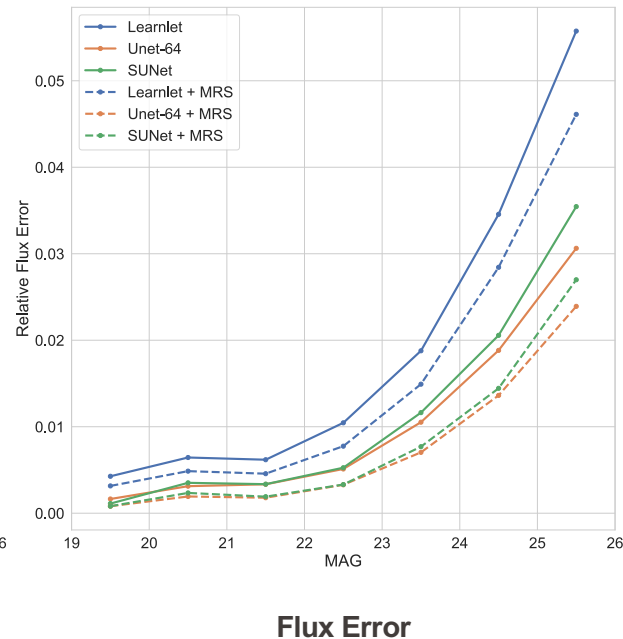
A



B



C



SSIM = 1: Identical  
SSIM = 0: Dissimilar

# Test on VLT Images

## EDisCS – the ESO distant cluster survey<sup>★,★★,★★★</sup>

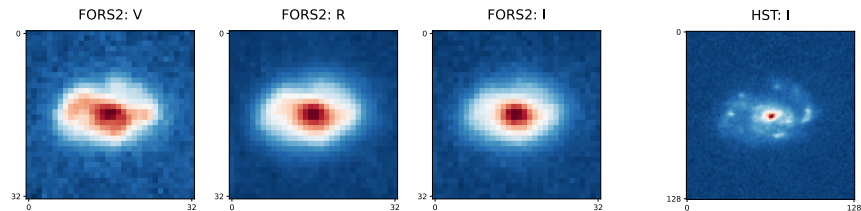
### Sample definition and optical photometry

S. D. M. White<sup>1</sup>, D. I. Clowe<sup>2</sup>, L. Simard<sup>3</sup>, G. Rudnick<sup>1</sup>, G. De Lucia<sup>1</sup>, A. Aragón-Salamanca<sup>4</sup>, R. Bender<sup>5</sup>, P. Best<sup>6</sup>, M. Bremer<sup>7</sup>, S. Charlot<sup>1</sup>, J. Dalcanton<sup>8</sup>, M. Dantel<sup>9</sup>, V. Desai<sup>8</sup>, B. Fort<sup>10</sup>, C. Halliday<sup>11</sup>, P. Jablonka<sup>12</sup>, G. Kauffmann<sup>1</sup>, Y. Mellier<sup>10,9</sup>, B. Milvang-Jensen<sup>5</sup>, R. Pelló<sup>13</sup>, B. Poggianti<sup>14</sup>, S. Poirier<sup>12</sup>, H. Rottgering<sup>15</sup>, R. Saglia<sup>5</sup>, P. Schneider<sup>16</sup>, and D. Zaritsky<sup>2</sup>

- All 84 cluster members at redshifts:  $z \approx 0.58$ ,  $z \approx 0.7$ , and  $z \approx 0.79$

Cluster IDs	Redshift ( $z_{cl}$ )	Number of samples ( $N_{cl}$ )
c11037.9-1243	0.5805	11
c11040.7-1155	0.7043	19
c11054.4-1146	0.6972	20
c11103.7-1245b	0.7031	6
c11216.8-1201	0.7955	28

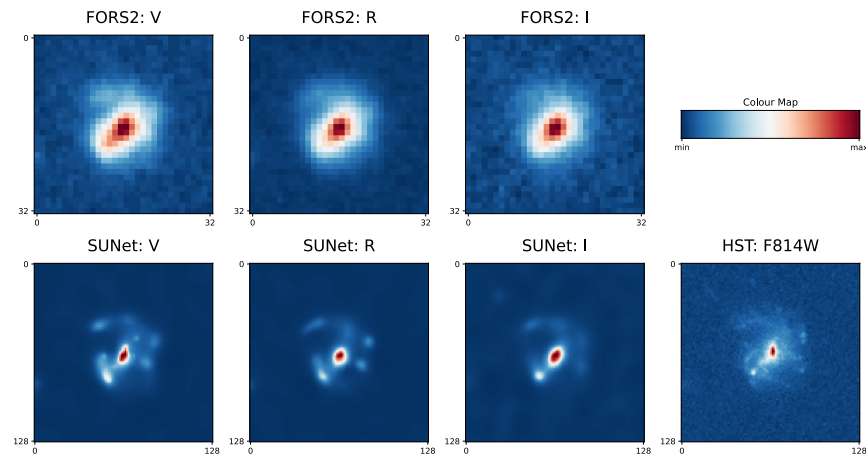
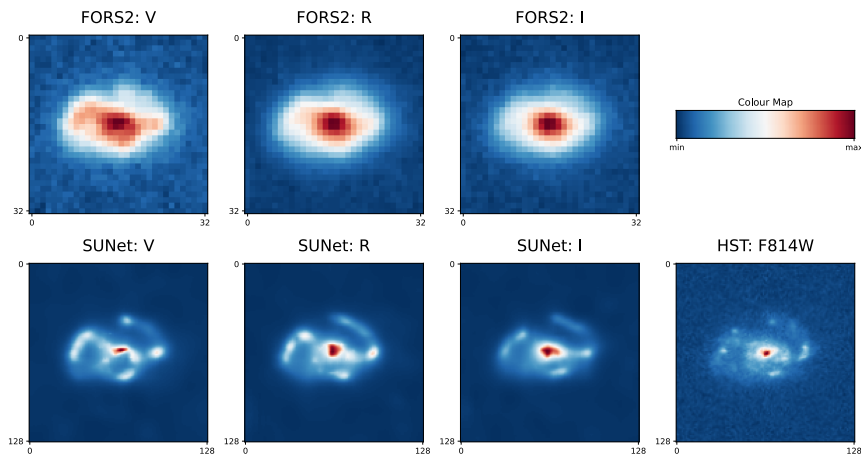
Table 1: Summary of the EDisCS clusters considered for analysis.



- Noisy images:** VLT FORS2 cutouts of  $32 \times 32$  pixels in  $V$  (555nm),  $R$  (655nm), and  $I$  (768nm) bands with resolution =  $0.2''$
- Ground truth:** HST ACS cutouts of  $128 \times 128$  pixels in the **F814W** filter ( $I$ -band) with resolution =  $0.05''$

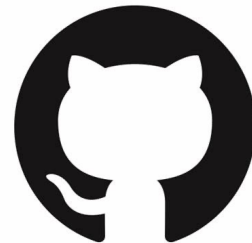


# Outputs



- Able to resolve small-scale structures and recover morphology
- Achieves a resolution close to HST
- Generalizes well to images with completely different noise properties than the training dataset

# Reproducible Research



- The ready-to-use version of our SUNet deconvolution method

<https://github.com/utsav-akhaury/SUNet/tree/main/Deconvolution>

- The repository fork of the SUNet code used for training the network

<https://github.com/utsav-akhaury/SUNet>

- Link to the trained SUNet weights

<https://doi.org/10.5281/zenodo.10287213>

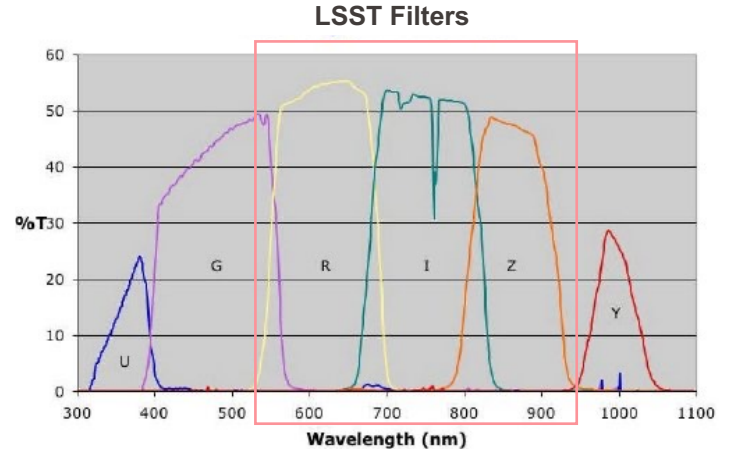
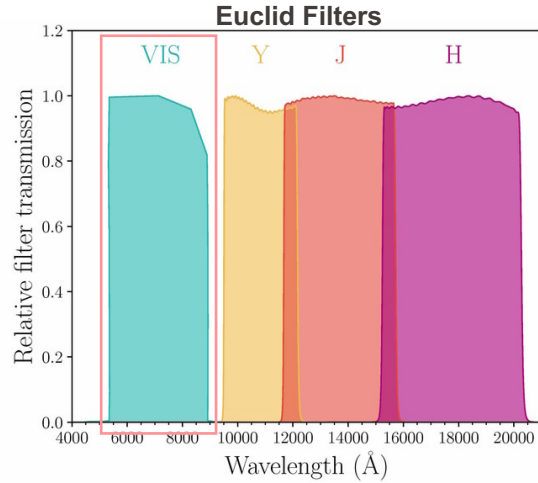
- The Learnlet and Unet-64 codes

<https://github.com/utsav-akhaury/understanding-unets/tree/candels>

▪

# Multi-channel Deconvolution

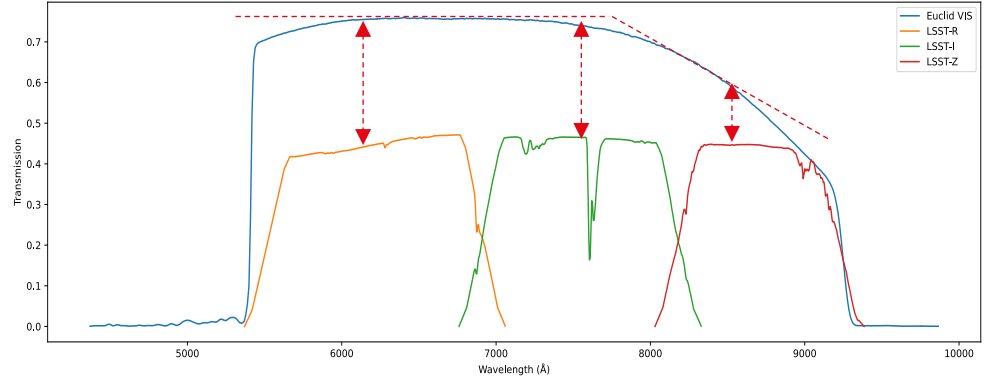
# Motivation



$$\mathbf{x}_{euc} = \alpha_R \mathbf{x}_R + \alpha_I \mathbf{x}_I + \alpha_Z \mathbf{x}_Z$$

Spectral Energy Distributions (SED)

$$\alpha_R, \alpha_I, \alpha_Z \in \mathbb{R}^n$$



# The Multi-channel Deconvolution Problem

## Model

$$\mathbf{y}_R = \mathbf{h}_R * \mathbf{x}_R^t + \eta_R$$

$$\mathbf{y}_I = \mathbf{h}_I * \mathbf{x}_I^t + \eta_I$$

$$\mathbf{y}_Z = \mathbf{h}_Z * \mathbf{x}_Z^t + \eta_Z$$

$$\mathbf{x}_{euc}^t = \alpha_R \mathbf{x}_R^t + \alpha_I \mathbf{x}_I^t + \alpha_Z \mathbf{x}_Z^t$$

$$\mathbf{y}_{euc} = \mathbf{h}_{euc} * \mathbf{x}_{euc}^t + \eta_{euc}$$

- Observed Noisy Images
- PSFs
- Ground Truth Images
- Additive Noise
- Spectral Energy Distributions (SED)

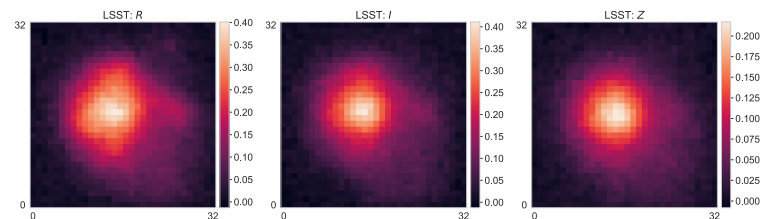
$$\mathbf{y}_R, \mathbf{y}_I, \mathbf{y}_Z \in \mathbb{R}^{n \times n}$$

$$\mathbf{h}_R, \mathbf{h}_I, \mathbf{h}_Z \in \mathbb{R}^{n \times n}$$

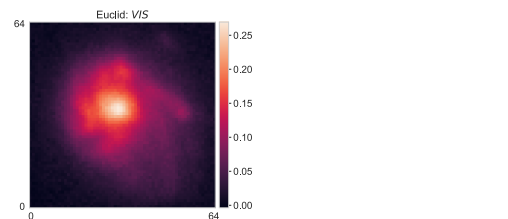
$$\mathbf{x}_R^t, \mathbf{x}_I^t, \mathbf{x}_Z^t \in \mathbb{R}^{n \times n}$$

$$\eta_R, \eta_I, \eta_Z \in \mathbb{R}^{n \times n}$$

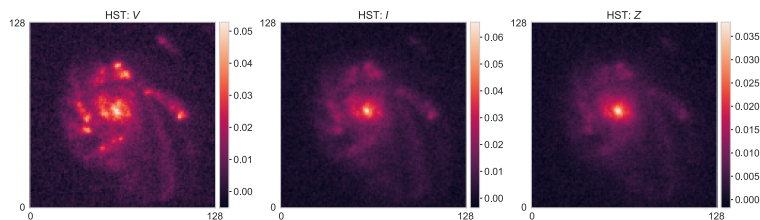
$$\alpha_R, \alpha_I, \alpha_Z \in \mathbb{R}^n$$



LSST  
0.2"



Euclid  
0.1"



HST  
0.05"

# The Loss Functions

$$L_R(\mathbf{x}_R) = \frac{1}{2} \left\| \frac{\mathbf{h}_R^* \mathbf{x}_R - \mathbf{y}_R}{\sigma_R} \right\|_F^2 + \lambda_{constr} \left\| \frac{\mathbf{h}_{euc}^* \sum_C \alpha_C \mathbf{x}_C - \mathbf{y}_{euc}}{\sigma_{euc}} \right\|_F^2$$

$$L_I(\mathbf{x}_I) = \frac{1}{2} \left\| \frac{\mathbf{h}_I^* \mathbf{x}_I - \mathbf{y}_I}{\sigma_I} \right\|_F^2 + \lambda_{constr} \left\| \frac{\mathbf{h}_{euc}^* \sum_C \alpha_C \mathbf{x}_C - \mathbf{y}_{euc}}{\sigma_{euc}} \right\|_F^2$$

$$L_Z(\mathbf{x}_Z) = \frac{1}{2} \left\| \frac{\mathbf{h}_Z^* \mathbf{x}_Z - \mathbf{y}_Z}{\sigma_Z} \right\|_F^2 + \lambda_{constr} \left\| \frac{\mathbf{h}_{euc}^* \sum_C \alpha_C \mathbf{x}_C - \mathbf{y}_{euc}}{\sigma_{euc}} \right\|_F^2$$

where

$$C \in \{R, I, Z\}$$

$$\lambda_{constr} \in \mathbb{R}_+$$

- Spectral Energy Distributions (SED)
- Noisemaps

$$\alpha_R, \alpha_I, \alpha_Z \in \mathbb{R}^n$$

$$\sigma_R, \sigma_I, \sigma_Z \in \mathbb{R}^{n \times n}$$

# Optimization

Loss Functions iteratively minimized using Gradient Descent

Step Sizes

$$\hat{\mathbf{x}}_{\{R,I,Z\}} = \underset{\mathbf{x}_{\{R,I,Z\}}}{\operatorname{argmin}} L_{\{R,I,Z\}}(\mathbf{x}_{\{R,I,Z\}})$$

$$\mathbf{x}_{\{R,I,Z\}}^{[k+1]} \leftarrow \mathbf{x}_{\{R,I,Z\}}^{[k]} - \beta_{\{R,I,Z\}} \nabla L_{\{R,I,Z\}}(\mathbf{x}_{\{R,I,Z\}}^{[k]})$$

$$\beta_R, \beta_I, \beta_Z \in \mathbb{R}^n$$

Gradients of the Loss Functions

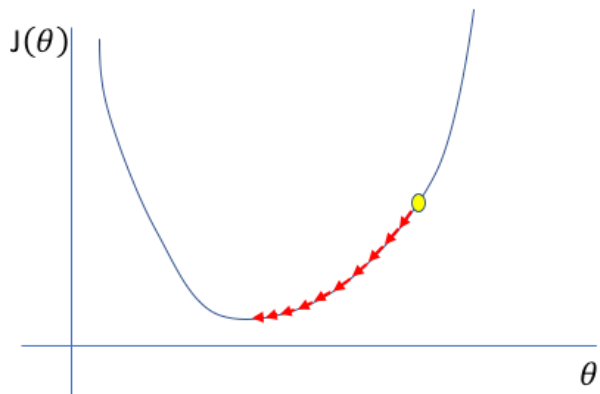
$$\nabla L_R(\mathbf{x}_R) = \frac{\mathbf{h}_R^\top * (\mathbf{h}_R * \mathbf{x}_R - \mathbf{y}_R)}{\|\sigma_R\|_F^2} + 2\lambda_{constr} \alpha_R \mathbf{h}_{euc}^\top * \left[ \frac{\mathbf{h}_{euc} * \sum_C \alpha_C \mathbf{x}_C - \mathbf{y}_{euc}}{\|\sigma_{euc}\|_F^2} \right]$$

$$\nabla L_I(\mathbf{x}_I) = \frac{\mathbf{h}_I^\top * (\mathbf{h}_I * \mathbf{x}_I - \mathbf{y}_I)}{\|\sigma_I\|_F^2} + 2\lambda_{constr} \alpha_I \mathbf{h}_{euc}^\top * \left[ \frac{\mathbf{h}_{euc} * \sum_C \alpha_C \mathbf{x}_C - \mathbf{y}_{euc}}{\|\sigma_{euc}\|_F^2} \right]$$

$$\nabla L_Z(\mathbf{x}_Z) = \frac{\mathbf{h}_Z^\top * (\mathbf{h}_Z * \mathbf{x}_Z - \mathbf{y}_Z)}{\|\sigma_Z\|_F^2} + 2\lambda_{constr} \alpha_Z \mathbf{h}_{euc}^\top * \left[ \frac{\mathbf{h}_{euc} * \sum_C \alpha_C \mathbf{x}_C - \mathbf{y}_{euc}}{\|\sigma_{euc}\|_F^2} \right]$$

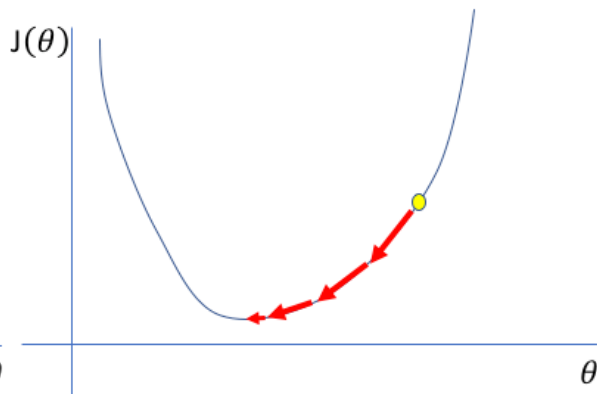
# Convergence Guarantee & Optimal step size

Too low



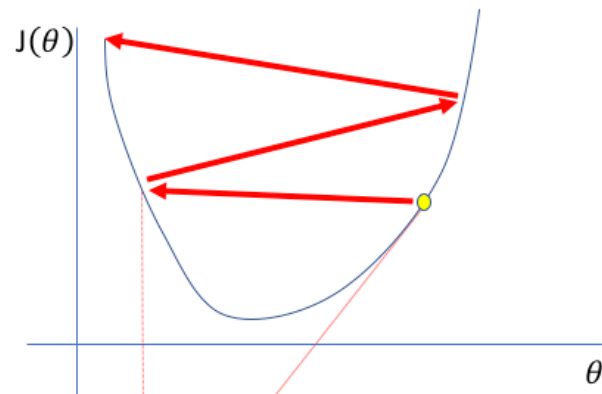
A small learning rate requires many updates before reaching the minimum point

Just right



The optimal learning rate swiftly reaches the minimum point

Too high



Too large of a learning rate causes drastic updates which lead to divergent behaviors



# Convergence Guarantee & Optimal step size

A function's gradient is Lipschitz continuous if

$$\|\nabla f(\mathbf{x}') - \nabla f(\mathbf{x})\| \leq C \|\mathbf{x}' - \mathbf{x}\|$$

where  $C$  is the Lipschitz constant

In our case

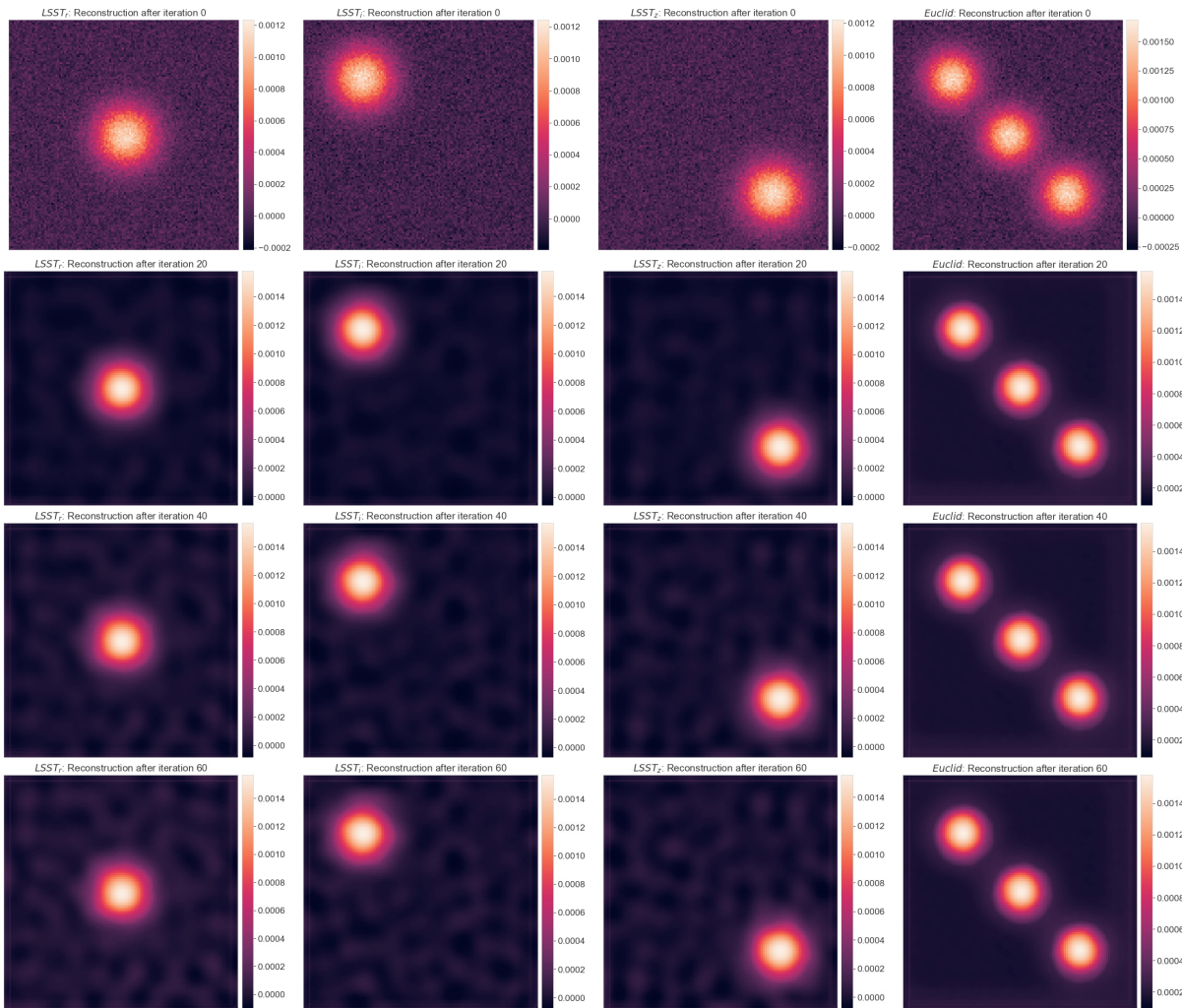
$$\|\nabla L_{\{R,I,Z\}}(\mathbf{x}'_{\{R,I,Z\}}) - \nabla L_{\{R,I,Z\}}(\mathbf{x}_{\{R,I,Z\}})\| \leq C_{\{R,I,Z\}} \|\mathbf{x}'_{\{R,I,Z\}} - \mathbf{x}_{\{R,I,Z\}}\|$$

Substituting the individual loss functions, we get

$$C_{\{R,I,Z\}} \geq \frac{\mathbf{h}_{\{R,I,Z\}}^\top * \mathbf{h}_{\{R,I,Z\}}}{\|\sigma_{\{R,I,Z\}}\|_F^2} + \frac{2\lambda_{constr}\alpha_{\{R,I,Z\}}^2 \mathbf{h}_{euc}^\top * \mathbf{h}_{euc}}{\|\sigma_{euc}\|_F^2}$$

**The Optimal Condition  
for Convergence**

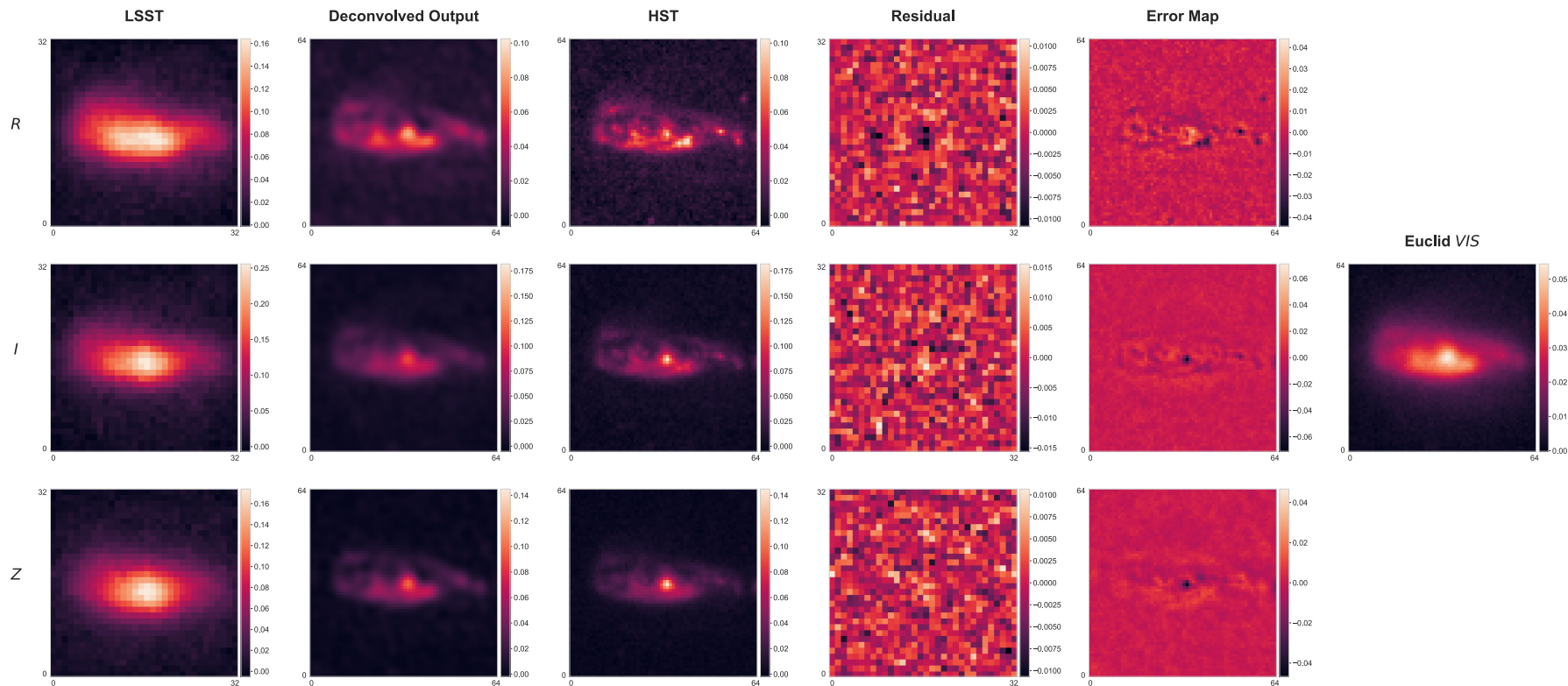
$$\beta_{\{R,I,Z\}} \leq \frac{1}{C_{\{R,I,Z\}}}$$



# Flux Leakage Test

- Assume 3 separately placed Gaussians in each channel (corresponding to LSST channels)
- The joint image (Euclid) is a linear sum of these channels
- No Flux Leakage from one channel to another

# A Deconvolved Object







**Thank You.**